CHARACTERIZATION OF SELECTED IRON ORE PROCESSING PLANT AT KUALA LIPIS, PAHANG, MALAYSIA

Muhammad Irman Khalif Ahmad Aminuddin, Zakaria Endut*, Fatin Nur Batrisha Amirah Ahmad Aminuddin and Talha Azlan

School of Materials and Mineral Resources Engineering, Universiti Sains Malaysia, Engineering Campus, 14300 Nibong Tebal, Penang, Malaysia.

*zakaria.endut@usm.my

Abstract. Iron ore from the processing plant at Kuala Lipis, Pahang, Malaysia, was characterized using four sample types: A (waste-cone crusher), B (ore-cone crusher), C (tailing), and D (concentration) to establish the most efficient and cost-effective processing procedures for its component ore or minerals. According to the PSD study, samples B and C were coarse-grained gravel. Meanwhile, sample D was categorized as fine-grained gravel. Optical microscopy reveals a dark grey to red granular Fe grain adhered to a quartz grain. The red stripe grains indicate the accumulation of iron ore, such as magnetite and hematite. SEM-EDX resulted in the iron concentration found to be Fe-Al-Si, while the XRD analysis supported this mineral identification as magnetite, hematite, zeolite, anorthite, andradite, and quartz are present as dominant phases. Following the XRF result, there was 26.48 % Fe, 40.86 % Fe, 31.1 % Fe and 89.24 % Fe in samples A, B, C, and D, respectively. Aluminium, silicon, and calcium are the following most abundant main elements. The Mozley table gravity separation was used to maximize the physical extraction of iron ore only from samples A, and C. Fe content for samples A and C was improved by 11.10 % and 7.02 %, respectively, using Mozley Table.

Keywords: Iron ore, characterization, Kuala Lipis, Pahang, Malaysia

Article Info

Received 11th October 2022
Accepted 14th December 2022
Published 23rd December 2022

ISSN: 1823-7010, eISSN: 2600-7444

Introduction

Malaysia's need for iron ore has continuously risen over the years. Malaysia produced roughly 2.42 million metric tonnes of iron ore in 2020 [1]. Pahang was reported to the one of the top iron ores in Malaysia [2], as the previously known Ulu Rompin iron deposits also known as Bukit Ibam, one of the high-grade primary ore bodies and superficial sheets of lateritic ore [3]. Nowadays, there are several abandoned and active iron mining sites in Pahang (Figure 1). The study area is an active iron ore processing plant located at Kuala Lipis district, Pahang, Malaysia. Magnetite ores are the primary ores produced from the mine and continued by the enrichment and recovery procedures to transform iron ore into ferrous metal. The characterization of iron ore is a profoundly important stage in examining the ore's grade, form, and properties before any beneficiation can occur. All the mineral's attributes must be established beforehand to apply relevant economic factors to help production planning [4]. The detailed data acquired throughout this research is beneficial in choosing the most pragmatic flow sheet for other iron and its constituent metals recovery stage. Proper and thorough research is executed to determine the iron ore characteristics for further information collection to aid in planning a practical ore extraction method and ore beneficiation process.

The industrial trend is to reduce the cost, both capital and operational, by maximizing the physical extraction of iron ore from processing plant. So, this paper aims to extract mineralogical characteristics information of iron ore from the selected iron ore processing plant, Kuala Lipis, Pahang. The data gathered throughout this project will be beneficial in determining the selection of the most efficient and cost-effective processing methods for its constituent metals or minerals.

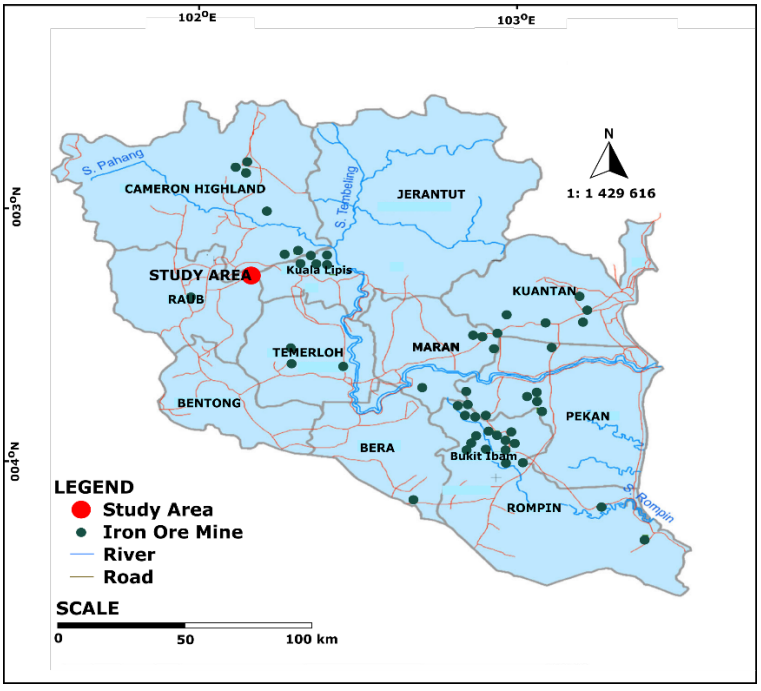

Figure 1: Map of active and abandoned iron ore mining sites in the state of Pahang [5]

Materials and Methods

Several fieldworks were carried out for iron ore sampling at the study area. The hand sample appears to range in pigment from light grey to dark grey, with grainy characteristics observed. Some parts appear brown, yellow, and black (Figure 2(a)). The formation of a reddish smudge indicates the presence of iron after scraping over andesite rock (Figure 2(b)). [6] reveals the Tembeling Andesite contained high amount of iron content when analysed using XRF and showed dust pigment probably iron ores in groundmass by petrographic analysis. Typically, the raw iron ore material dug from the mining area is pulverized using various crushers and refined through the gravitational segregation, magnetic separation, and flotation of ore minerals, followed by smelting or palletizations of iron [7-10].

Figure 3 shows the simple flowchart of the processing plant at study area. There are four sample types taken for further analyses in this study, namely A (waste product of cone crusher), B (ore product from cone crusher), C (tailing of magnetic separator) and D (concentrate of magnetic separator). Further mineral classification studies, including PSD, XRD, XRF, and SEM-EDX, must be carried out before any conclusion determining the kind of mineral found.

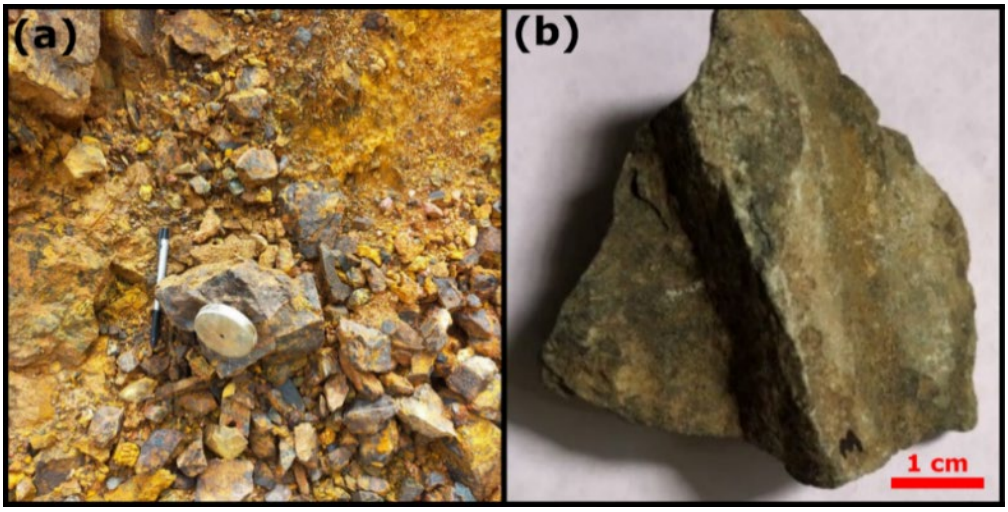

Figure 2: The ore sample (a) outcrop sample from Benta Mine, Pahang, Malaysia and (b) hand sample, which is commonly pebble to boulder size

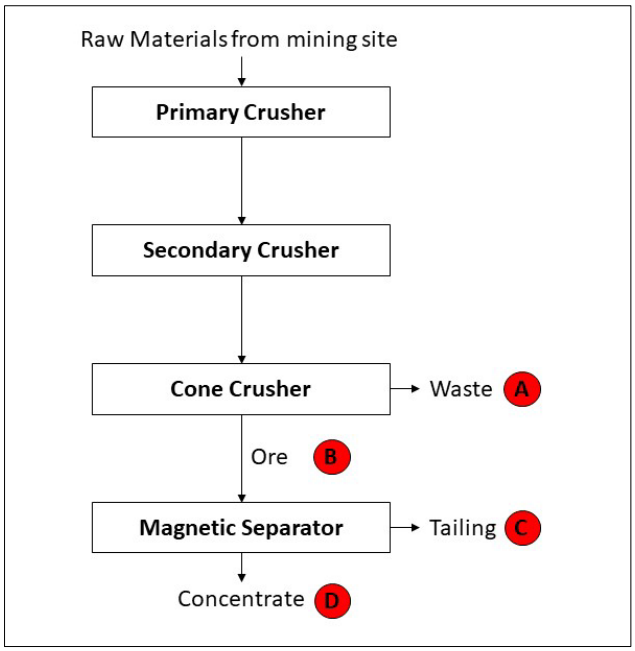

Figure 3: Flowchart of the selected iron ore processing plant, Kuala Lipis, Pahang, Malaysia

Results and Discussion

Particle Size Distribution

The product's particle size after the size reduction procedure is significant in evaluating the mineral liberation rate and the finished product's performance after being ground. It is also used to identify the best input amount for peak performance of the beneficiation process and to discover the material size categories at which deficits occur during the beneficiation procedure so that this issue can be reduced [11]. The mean particle size shows the uniformity of the particle system. The system comprises several distinct particle sizes and shapes. In this research, the size of the product was determined using the technique of sieving after crushing. The crushed product was sieved into various sizes following [12] procedure. Only sample A (waste from cone crusher) was not performed in this analysis because this sample is considered waste and will not be processed in this processing plant. The findings of the size study for samples B, C and D are shown in Figure 4(a), (b) and (c), respectively. Figure 4(a) shows cumulative passing against aperture size shows that d_{10}, d_{50}, and d_{90} are 0.44 mm, 0.60 mm, and 5.17 mm for sample B, respectively. This assumes that 10 % of the sample size is less than 0.44 mm and 90 % of the sample size is more than 0.44 mm. Apart from that, the sample's median diameter is 0.6 mm. This implies that half of the sample size is more than 0.6 mm, and the other half is less than 0.6 mm. 90 % of the sample size is less than 5.17 mm, whereas 10 % is more significant than 5.17 mm, according to d_{90}.

Figure 4(b) shows cumulative passing against aperture size shows that d_{50} and d_{90} are 0.17 mm and 1.42 mm for sample C, respectively. This assumes that 50 % of the sample size is less than 0.17 mm and 90 % of the sample size is more than 0.17 mm. Apart from that, the sample's median diameter is 0.17 mm. This implies that half of the sample size is more than 0.17 mm, and the other half is less than 0.17 mm. 90 % of the sample size is less than 2.5

mm, whereas 10% is more significant than 1.4 mm, according to d_{90}. Figure 4(c) shows cumulative passing against aperture size, showing that d_{50} and d_{90} are 2.42 mm and 16.6 mm for Sample D, respectively. This assumes that 50 % of the sample size is less than 2.42 mm and 90 % of the sample size is more than 16.6 mm. Apart from that, the sample's median diameter is 2.42 mm. This implies that half of the sample size is more than 2.42 mm, and the other half is less than 2.42 mm. 90 % of the sample size is less than 16.6 mm, whereas 10 % of the sample size is more significant than 16.6 mm, according to d_{90}. The findings show that sample B is in course gravel since sample B's range is between 0.44 mm and 5.17 mm. Same as sample B, sample C is categorized as coarse gravel since it ranges between 0.17 mm and 1.40 mm, whereas sample D's distribution is between 2.42 mm and 16.60 mm, which is in the fine gravel category. The soil classification system follows [13].

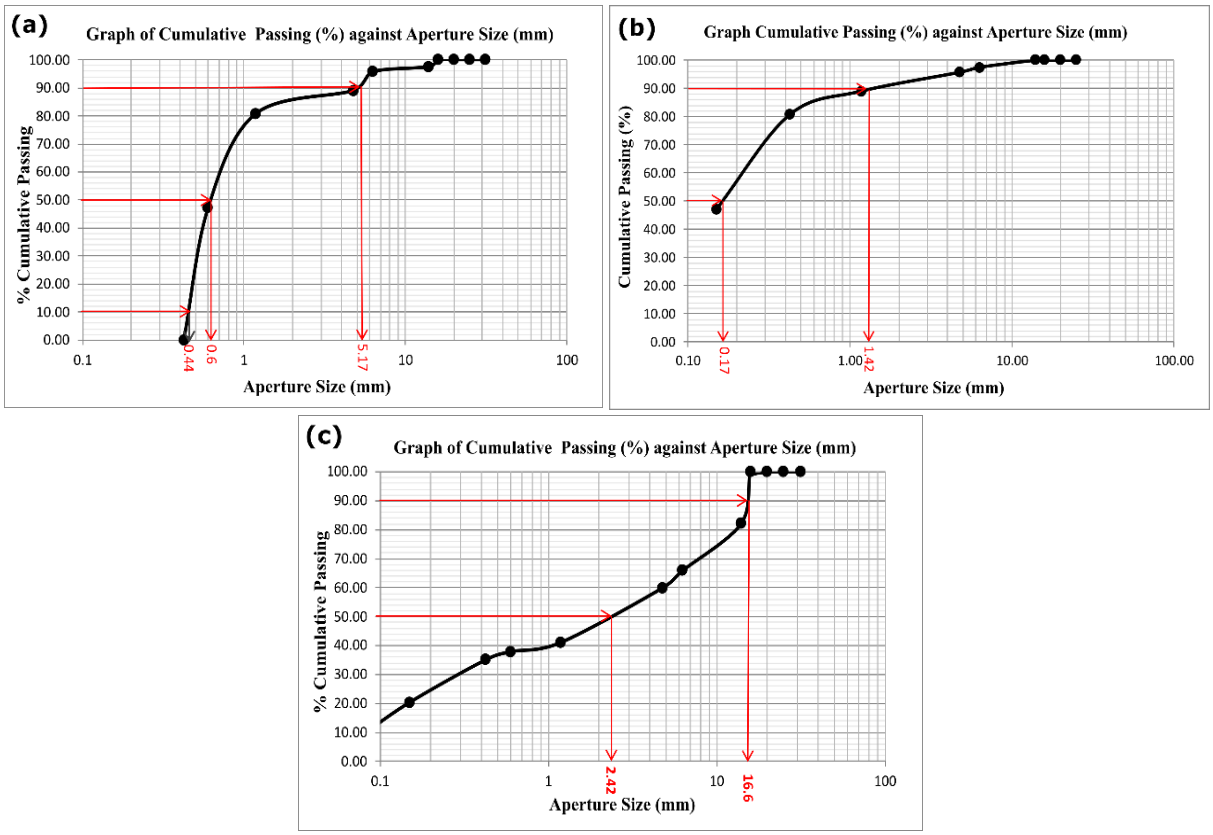

Figure 4: The particle size distribution results. (a) sample B, (b) sample C and (c) sample D

Ore Mineralogy

Iron ore rocks from the mine were prepared for the polish section and based on the image generated by the optical microscope, the interpreted mineral that exists in the iron ore sample follows [14,15] is quartz, magnetite, sulphur, and hematite (Figure 5). The free particles of magnetite minerals as shown in Figure 5(a). Figure 5(b) indicated the presence of hematite mineral in orange-coloured and showed that the Fe mineral interlocks with quartz. Figure 5(c) the iron can be seen under the microscope due to its size and colour, which are larger and black coloured, bolder than any other minerals. The quartz mineral is presented as shiny white particles, whereas the black-coloured mineral is stipulated as magnetite. The mineral granules are irregular in shape, and most minerals are still interlocking with another mineral particle. Based on Figure 5(d), iron ore minerals are present; the orange-coloured

mineral is considered hematite due to its colour and the higher probability [15] that it has to co-exist with magnetite ore. In addition, quartz and silica normally associate together with any other ores as the gangue mineral.

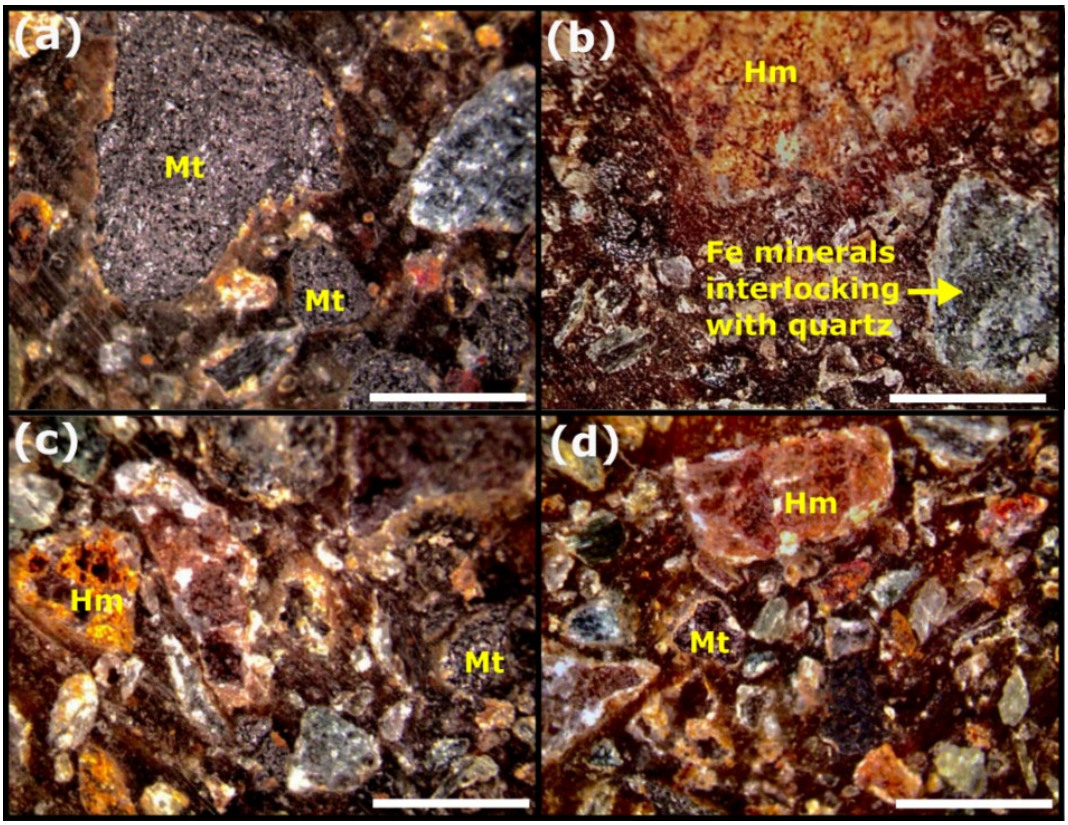

Figure 5: Image of optical microscope for iron ore minerals from cone crusher (sample B). The scale bar (red colour) indicates 10µm. *Abbreviations: Mt-magnetite, Hm-hematite, and Fe-iron*

The raw data for waste rock from the cone crusher (sample A) is shown in Figure 6. According to the SEM photomicrograph observation, the structural surface of the sample is not smooth. The sample contains spots in three different colours: light grey, grey, and dark grey. Apart from that, the dark grey portion appears more significant than the dark grey in the sample, indicating that the impurities removal procedure for highly complicated. The <100 µm size of the magnetite and free particles of Fe minerals are still present in this sample, and it can be extracted more from this sample. The data from XRD for this sample as shown in Figure 7, the magnetite and quartz were dominant in sample A.

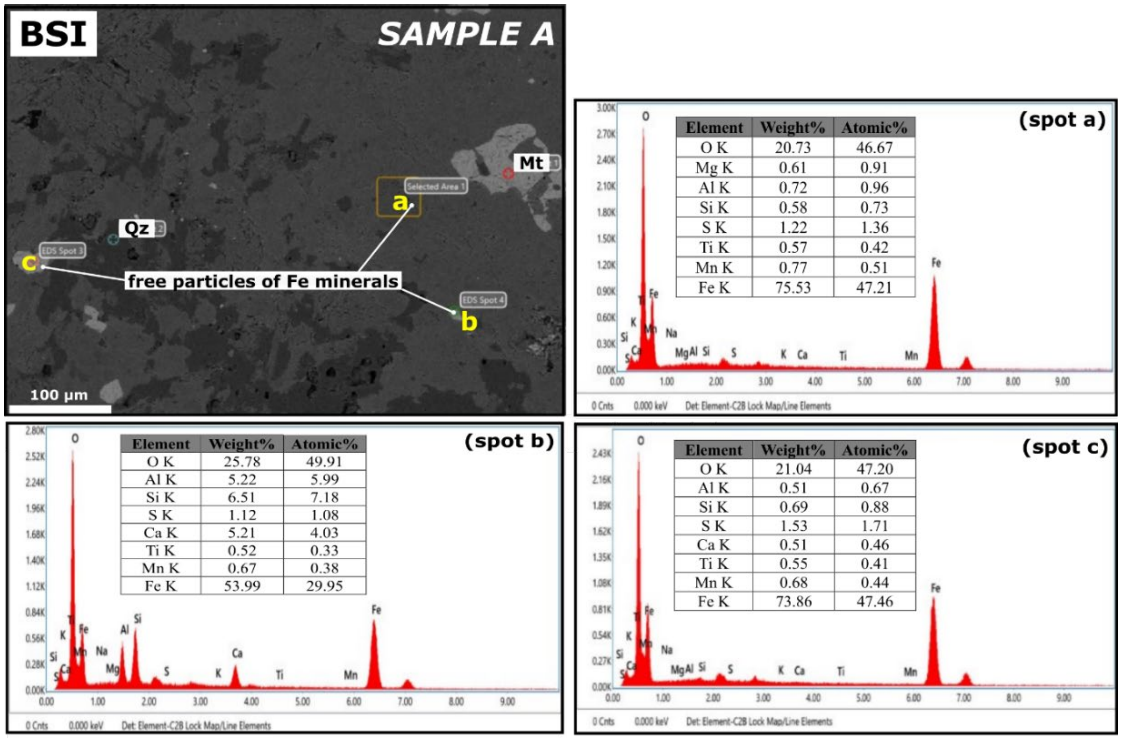

Figure 6: Back scattered image (BSI) and SEM-EDX spot results of waste from cone crusher sample (sample A)

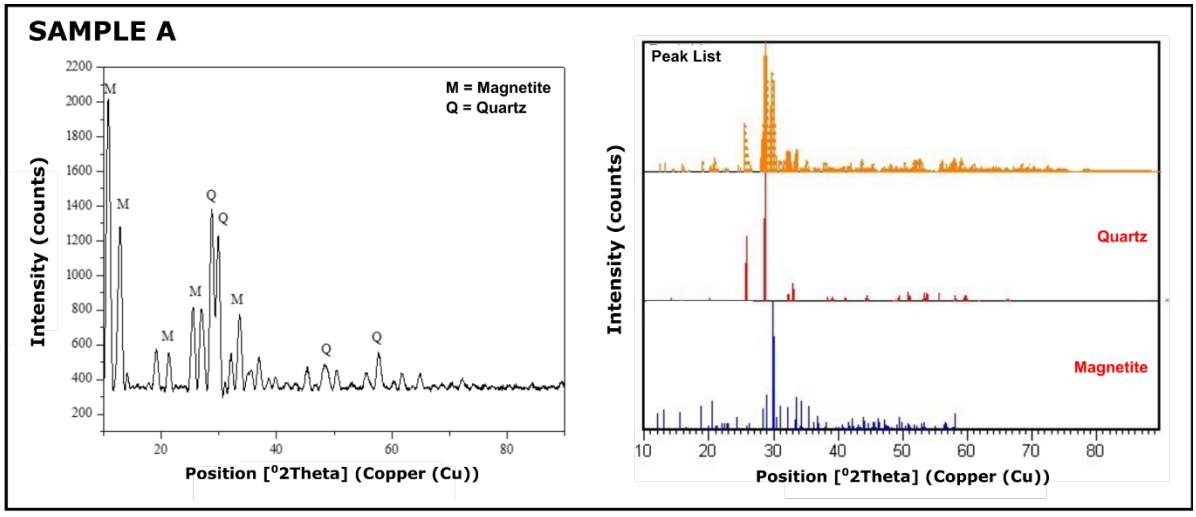

Figure 7: XRD pattern for sample A

According to Figure 8, the SEM photomicrograph of iron ore from the cone crusher (sample B) consists of three distinct shades of grey: light grey, grey, and dark grey. Regarding the EDX spectrum obtained from the highlighted spot in the SEM photomicrograph, we may recognize the elements included in the sample as Fe, Ti, O, Al, Si, P, S, Ca, Cr and Mn. It is known from the data that there are elements in the sample that are interlocked with each other. The size of the minerals shown from BSI for this sample is much

bigger than the size from sample A. Whilst in XRD pattern for this sample, zeolite and magnetite existed in sample B (Figure 9).

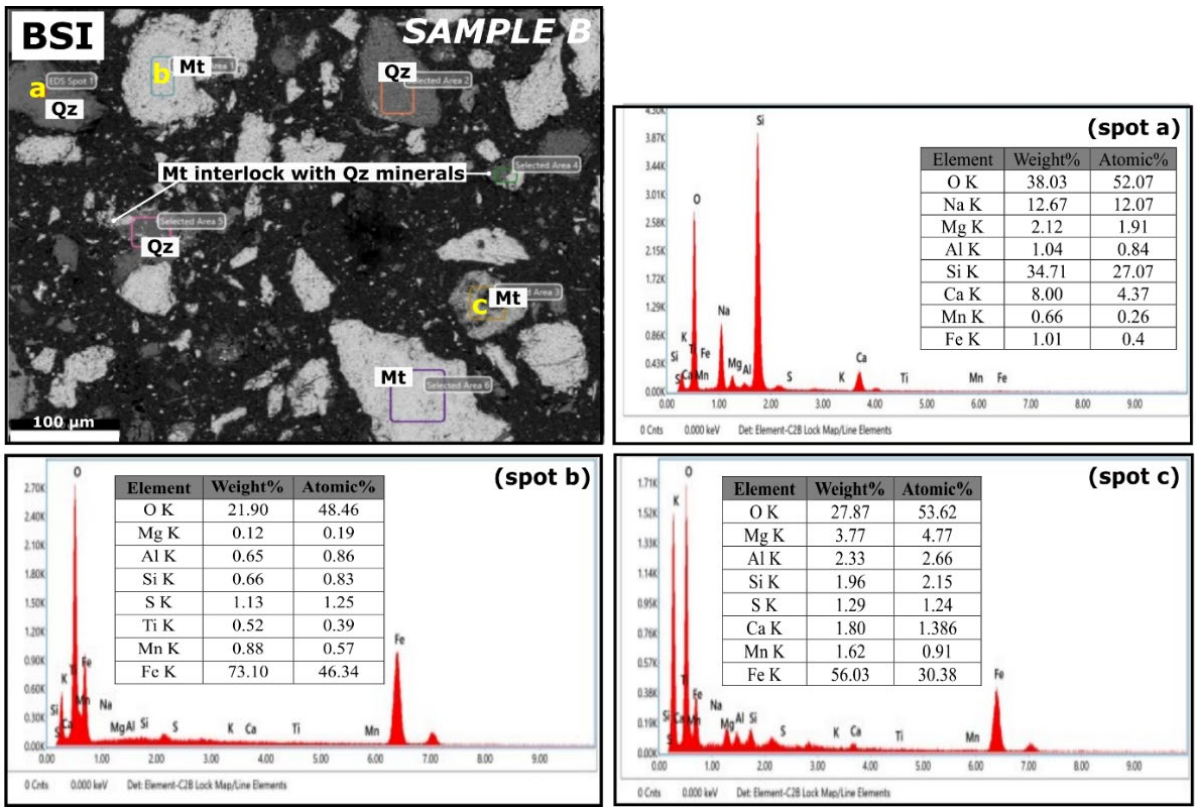

Figure 8: Back scattered image (BSI) and SEM-EDX spot results of iron ore from cone crusher sample (sample B)

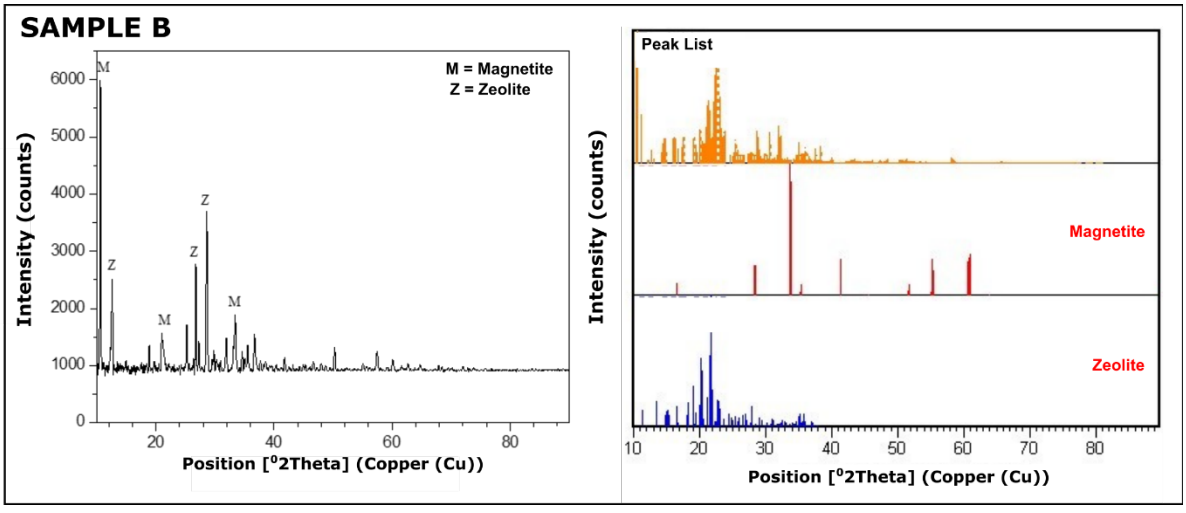

Figure 9. XRD pattern for sample B

According to Figure 10, the SEM photomicrograph of tailings (sample C) reveals only two different shades of grey: light grey and dark grey. Concerning the EDX spectrum obtained from the highlighted spot in the SEM photomicrograph, the elements included in the sample may be recognized as Fe, Ti, O, Al, Si, P, S, Ca, Cr and Mn. It is known from the data that there are elements in the sample that are interlocked with each other. The sample's

surface is not smooth. Besides, the light grey region in the sample is smaller than the dark grey, indicating that the procedure for eliminating impurities is quite complicated. Generally, the unwanted minerals are the most significant presence but still have the Fe minerals that can be extracted more. For XRD pattern shown magnetite and anorthite phases in sample C (Figure 11).

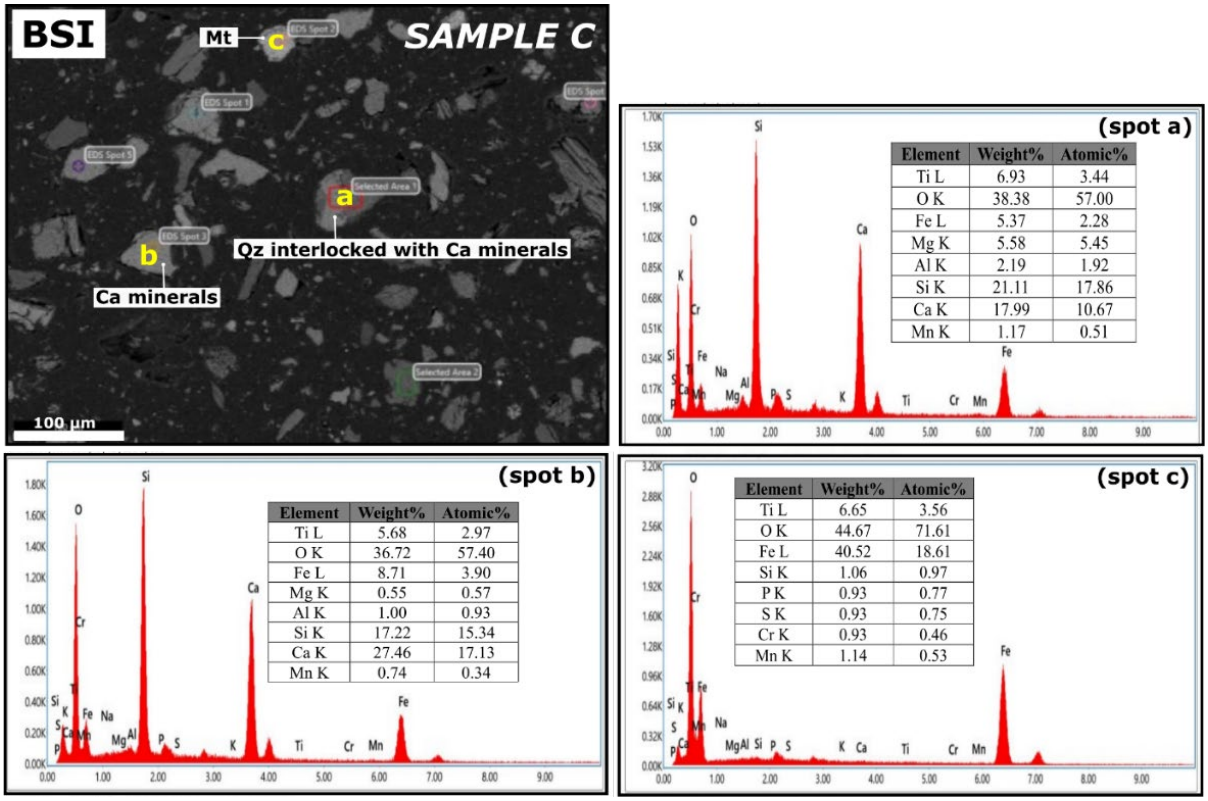

Element	Weight%	Atomic%
Ti L	6.93	3.44
O K	38.38	57.00
Fe L	5.37	2.28
Mg K	5.58	5.45
Al K	2.19	1.92
Si K	21.11	17.86
Ca K	17.99	10.67
Mn K	1.17	0.51

Element	Weight%	Atomic%
Ti L	5.68	2.97
O K	36.72	57.40
Fe L	8.71	3.90
Mg K	0.55	0.57
Al K	1.00	0.93
Si K	17.22	15.34
Ca K	27.46	17.13
Mn K	0.74	0.34

Element	Weight%	Atomic%
Ti L	6.65	3.56
O K	44.67	71.61
Fe L	40.52	18.61
Si K	1.06	0.97
P K	0.93	0.77
S K	0.93	0.75
Cr K	0.93	0.46
Mn K	1.14	0.53

Figure 10: Back Scattered Image (BSI) and SEM-EDX spot results of tailings from magnetic separator (sample C)

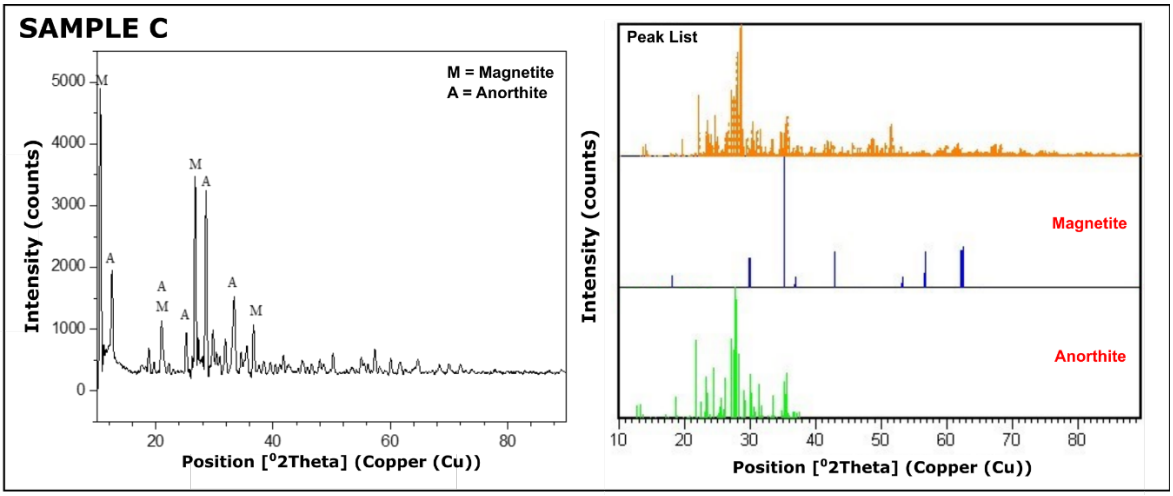

Figure 11: XRD pattern for sample C

According to Figure 12, the BSI for concentrate (sample D) reveals the majority magnetite minerals presence in the concentrate sample in which are interlocked with each other and quartz minerals. Generally, the iron ore minerals are the most significant presence but still have the unwanted quartz minerals. For XRD pattern shown magnetite and andradite phases in sample D (Figure 13).

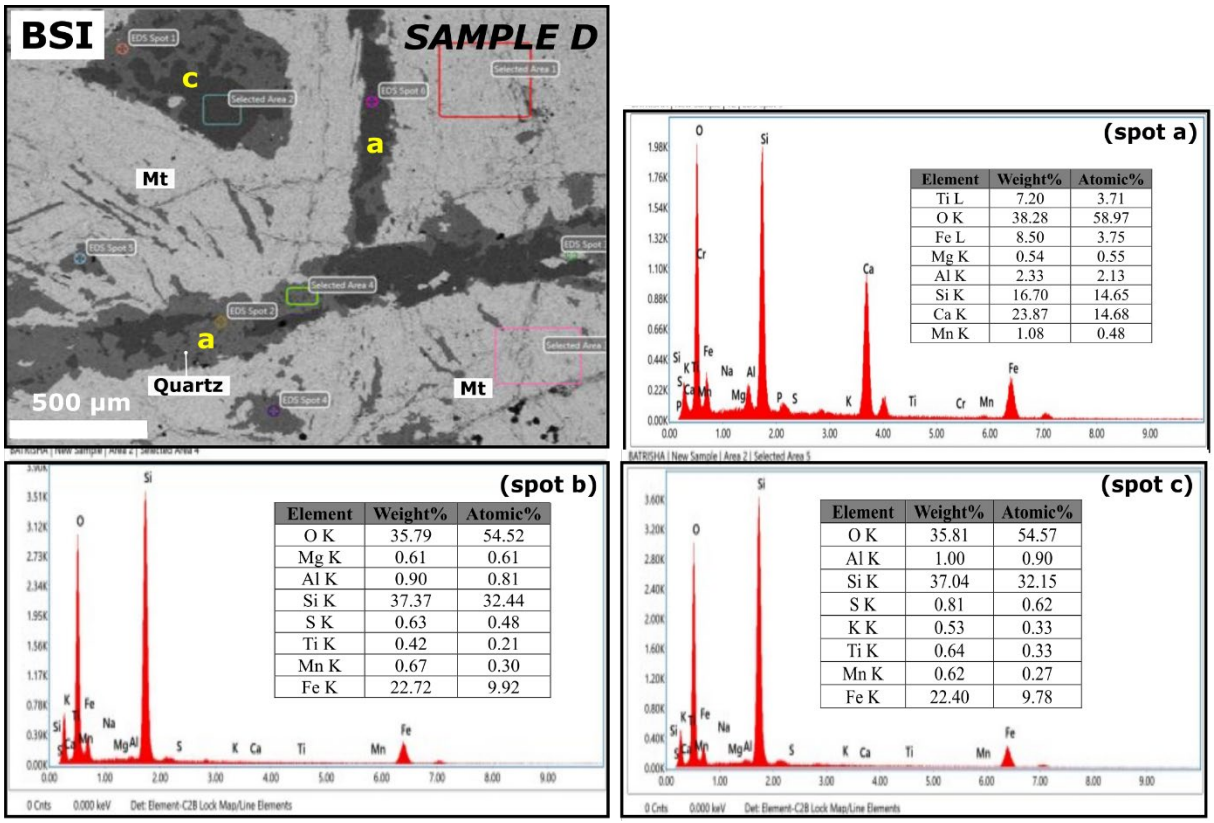

Element	Weight%	Atomic%
Ti L	7.20	3.71
O K	38.28	58.97
Fe L	8.50	3.75
Mg K	0.54	0.55
Al K	2.33	2.13
Si K	16.70	14.65
Ca K	23.87	14.68
Mn K	1.08	0.48

Element	Weight%	Atomic%
O K	35.79	54.52
Mg K	0.61	0.61
Al K	0.90	0.81
Si K	37.37	32.44
S K	0.63	0.48
Ti K	0.42	0.21
Mn K	0.67	0.30
Fe K	22.72	9.92

Element	Weight%	Atomic%
O K	35.81	54.57
Al K	1.00	0.90
Si K	37.04	32.15
S K	0.81	0.62
K K	0.53	0.33
Ti K	0.64	0.33
Mn K	0.62	0.27
Fe K	22.40	9.78

Figure 12. Back Scattered Image (BSI) and SEM-EDX spot results of concentrate from magnetic separator (sample D)

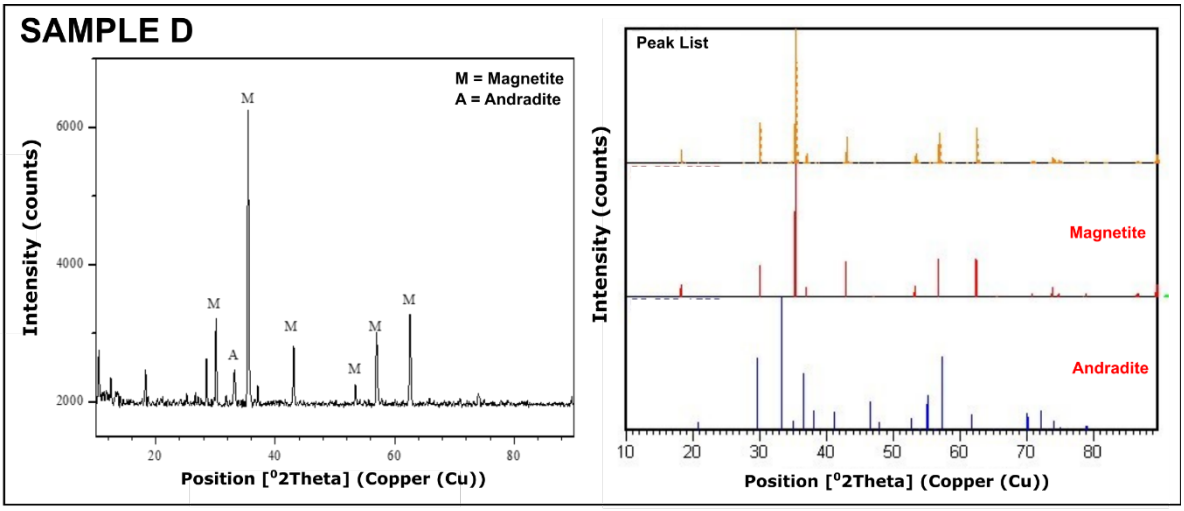

Figure 13. XRD pattern for sample D

Chemical Composition

Four samples were evaluated with XRF analysis to identify the chemical makeup, particularly the iron oxide and silica content. The approximate proportion of each composition that exists in all samples is determined in Table 1.

Table 1: The estimated result for XRF analysis

Chemical Composition	Element	Mass (%)			
		Sample A (Waste from cone crusher)	Sample B (Ore from cone crusher)	Sample C (Tailings)	Sample D (Concentrate)
Al_2O_3	Al	8.600	15.000	12.000	5.400
SiO_2	Si	35.400	30.000	37.200	2.600
SO_2	S	0.280	0.380	0.610	0.000
K_2O	K	0.140	0.110	0.140	0.000
CaO	Ca	27.080	12.50	16.930	1.980
TiO_2	Ti	0.451	0.365	0.366	0.000
V_2O_5	V	0.034	0.032	0.024	0.025
Cr_2O_3	Cr	0.021	0.000	0.017	0.039
MnO	Mn	1.000	0.949	1.050	0.209
Fe_3O_4	Fe	26.480	40.860	31.100	89.240
CuO	Cu	0.034	0.045	0.046	0.037
ZnO	Zn	0.030	0.026	0.020	0.000
GeO_2	Ge	0.000	0.014	0.013	0.000
Rb_2O	Rb	0.010	0.015	0.0079	0.038
SrO	Sr	0.060	0.033	0.054	0.005
Y_2O_3	Y	0.000	0.000	0.011	0.000
ZrO_2	Zr	0.017	0.026	0.024	0.000
MoO_3	Mo	0.008	0.009	0.007	0.000
In_2O_3	In	0.160	0.100	0.210	0.000
HgO	Hg	0.032	0.020	0.010	0.000
PbO	Pb	0.090	0.000	0.00	0.000

According to the data, the key elements found in samples B and D are Fe, which account for 40.86 and 89.24 per cent of the content. Meanwhile, the main element found in samples C and A is Si at 37.2 and 35.4 per cent by mass, respectively. All samples also detected other components, including Al, Si, Ti, V, Cr, Ni, Cu, Zn, As, Zr, and Pb. But all those compositions were detected at a low concentration due to their portions being less than 1 %. The results of the XRF test are shown graphically (Figure 14). According to the Figure 14(a), sample A, B, C and D have 26.48 %, 40.86 %, 31.10 %, and 89.24 % of the required Fe. In comparison, the three top elements present in the samples are silicon (Figure 14(b)),

calcium (Figure 14(c)), and aluminium (Figure 14(d)). The existence of trace elements, such as Al, Si, Ti, K, Ca, and S, is a possible sign of disintegration. Because these elements are often found in the region where the sample was taken, it shows that weathering occurred in that location. According to [4] the medium iron grade, which is economical to mine, has a Fe content ranging between 62-65 %. Very high levels of Fe are included in sample D, which is 89.24 %. This suggests that the land in this region may be profitable to mine.

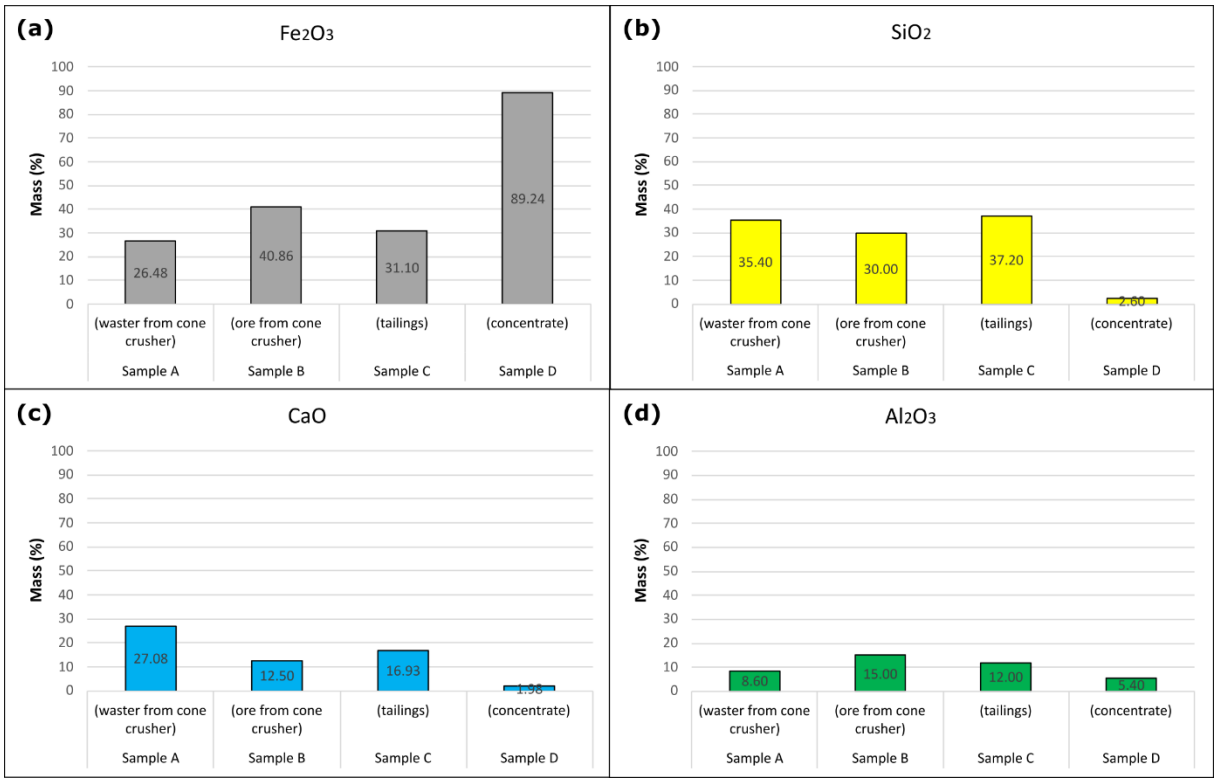

Figure 14. XRF results were plotted in graph of (a) Fe_2O_3 composition against Mass (%), (b) SiO_2 composition against Mass (%), (c) CaO composition against Mass (%) and (d) Al_2O_3 composition against Mass (%) for 4 studied samples

Mineral Concentration

The still presence of iron ore in sample A and C was led to mineral concentrations by using mozley table gravity separation to maximize the physical extraction of iron ore from the Kuala Lipis processing plant. The XRF results reveal 26.48 % and 31.10 % of iron content in sample A and C, respectively (Figure 14(a)) and relatively contained same amount of the SiO_2 (Figure 14(b)) for both sample A and C. Separation can be achieved on mozley table between iron dan silica minerals as these two minerals have a reasonable difference in specific gravity. Calculated concentration criterion (Cc) between these two minerals is 2.96. With a concentration criterion of 2.5 or more rapid separation efficiency is comparatively simple [11].

All the samples used by the Mozley Table use the same parameter settings. The flow rate and duration of the watering operation remain consistent. At the specified period, the amount of time each sample will be run on the Mozley Table is four minutes. The information in Table 2 comes from the results of the mineral concentration procedure.

According to the results, sample A and D have 33.50% and 42.50% of concentrate, respectively. The amount of concentrate in the sample D is slightly higher than in sample A. There were some portions of samples that were lost during the mineral processing procedure. The loss was due to extra fine particles becoming slime during the mineral concentration process.

Table 2: Result for mineral concentration by using Mozley Table

Sample	Weight sample (g)	Concentrate (g)	Tailing (g)	Losses (g)	% Concentrate
A	200.37	67.12	114.42	18.83	33.50
C	200.30	84.53	98.79	16.68	42.20

Conclusions

This paper presented the characterization of selected iron ore from processing plant at Kuala Lipis, Pahang, Malaysia for possible recovery of remaining elements, especially the iron ore. When compared to the ideal particle size distribution graph for grain classification, it can be deduced that both sample B and C are coarse-grained gravel and sample D is categorized as fine-grained gravel. D10, D50, and D90 were used in the calculations, resulting in this conclusion. Tailings sample has particles that vary from 0.17 mm to 1.40 mm in size. The range for concentrate sample is 2.42 mm to 16.6 mm and the last one, iron ore from cone crusher is between 0.44 mm and 5.17 mm. Ore Visual assessment found the rock surface has an uneven structure with an average size of-50 mm. Fe-minerals such as magnetite and hematite are discovered in the ore mineralogy by polished section study and supported through SEM-EDX, the iron concentrate was determined to be Fe-Al-Si. A granular Fe grain with a dark grey to red colour has been found interlocking with quartz through visual microscopy. The iron ore itself is shown by the red streak in the image. Meanwhile, XRD magnetite, quartz, anorthite, zeolite, and andradite are the dominant phases present according to the XRD pattern. The XRF examination showed the components contained in the samples. In Sample A, B, C and D, there is 26.48 % Fe, 40.86 % Fe, 31.1 % Fe and 89.24 % Fe correspondingly. Trace amounts of these additional elements (Al, Si, Ti, and Ni) were discovered, but they are below the one percent threshold. The discovery that magnetite was found in all samples led to the conclusion that iron oxide was contained in the ore. More recovery from the Mozley Table specific gravity separation in order to maximize the best physical processing of iron ore as sample A and C have 33.50 % and 42.50 % of concentrate, respectively.

Acknowledgements

Authors are in debt to the team of the project ‘Characterization of Iron Ore from Kuala Lipis, Pahang, Malaysia’ for the logistic and research support.

Author Contributions

All authors contributed toward data analysis, drafting and critically revising the paper and agree to be accountable for all aspects of the work.

Disclosure of Conflict of Interest

The authors have no disclosures to declare.

Compliance with Ethical Standards

The work is compliant with ethical standards

References

[1] World Bureau Of Metal Statistics (2021). [Online]. [Accessed 12nd August 2022]. Available from Statista Website: https://www.statista.com/statistics/1132484/malaysia-iron-ore-production

[2] Majid, A.A., Shaharudin, H.M., Alias, S., Adnan, E., Hassan, A.I.A. & Ali M.Z. (2013). Malaysia Mining Industry. (Report, Minerals and Geoscience Department of Malaysia).

[3] Bean, J.H. (1975). The Iron Ore Deposits of Ulu Rompin, Malaya. (PhD thesis, Durham University, England) pp. 1-382.

[4] Kiptarus, J.J., Muumbo, A.M., Makokha, A.B. & Kimutai, S.K. (2015). Characterization of Selected Mineral Ores in the Eastern Zone of Kenya: Case Study of Mwingi North Consituency in Kitui County. *International Journal of Mining Engineering and Mineral Processing,* 4(1), 8-17.

[5] Madzin, Z., Kusin, F.M., Yusof, F.M. & Muhammad, S.N. (2017). Assessment of Water Quality Index and Heavy Metal Contamination in Active and Abandoned Iron Ore Mining Sites in Pahang, Malaysia. *MATEC Web of Conferences,* 103, 1-9.

[6] Willbourn, E.S. (2017). III-The Pahang Volcanic Series. *Geological Magazine.* Published online by Cambridge University Press. 447-463.

[7] Morkun, V., Tron, V. & Zymohliad, V. (2022). Modelling of Iron Ore Processing in Technological Units Based on the Hybrid Approach. *Acta Mechanica et Automatica,* 16(1), 82-90.

[8] Bertrand, C., Bazin, C. & Nadeau, P. (2018). Simulation of a Dry Magnetic Separation Plant. *Advances in Metallurgical and Material Engineering,* 1(1), 15-28.

[9] Nomura, T., Yamamoto, N., Fujii, T. & Takiguchi, Y. (2015). Beneficiation Plants and Pelletizing Plants for Utilizing Low Grade Iron Ore. *Kobelco Technology Review,* 33, 8-15.

[10] Dahe, X. (2003). Slon Magnetic Separator Applied to Upgrading The Iron Concentrate. *Physical Separation in Science and Engineering,* 12(2), 63-69.

[11] Will, B.A. & Napier-Munn, T.J. (2006). *Wills' Mineral Processing Technology.* 7th edition (Elsevier Ltd) pp. 225-244.

[12] Dishman, K.L. (2006). *Sieving in Particle Size Analysis.* Encyclopedia of Analytical Chemistry. 2nd edition (John Wiley & Sons Ltd) pp. 1-5.

[13] Carter, M. & Bentley, S.P. (2016). *Soil Properties and their Correlations*. 2nd edition (John Wiley & Sons). pp. 1-67.

[14] Craig, J.R. & Vaughn, D.J. (1994). *Ore Microscopy and Ore Petrography.* 2nd edition (John Wiley & Sons) pp. 1-305.

[15] Marshall, D., Anglin, C.D. & Mumin, H. (2004). *Ore Mineral Atlas.* (Geological Association of Canada – Mineral Deposits Division, Canada). pp. 1-126.